frontiers in Environmental Chemistry

ORIGINAL RESEARCH
published: 01 November 2021
doi: 10.3389/fenvc.2021.706254

Amino-Thiol Bifunctional Polysilsesquioxane/Carbon Nanotubes Magnetic Composites as Adsorbents for Hg(II) Removal

Ting Xu, Rongjun Qu, Ying Zhang, Changmei Sun, Ying Wang, Xiangyu Kong, Xue Geng and Chunnuan Ji*

School of Chemistry and Materials Science, Ludong University, Yantai, China

Amino-thiol bifunctional polysilsesquioxane/carbon nanotubes (PSQ/CNTs) magnetic composites were prepared by sol-gel method with two types of functional siloxanes coating on carboxyl CNTs simultaneously. The composites were served as efficient adsorbents for removing Hg(II) in aqueous solution and the adsorption properties were investigated systematically. The optimal pH of bifunctional composites for Hg(II) removal is at pH 4.5. The thermodynamic fitting curves are more consistent with the Langmuir model and the adsorption capacities of the bifunctional composites for Hg(II) varied from 1.63 to 1.94 mmol g^{-1} at 25°C according to the Langmuir model. The kinetics curves are more fitted to the pseudo-second-order model and the composites could selectively adsorb Hg(II) in a series of binary metal ions solution. The elution regeneration tests showed that the adsorption rate could still reach 78% after repeat cycle three times. It is expected that the bifunctional PSQ/CNTs magnetic composites can be potentially applied to remove low concentration Hg(II) from waste water.

Keywords: polysilsesquioxane, CNTs, adsorption, Hg(II), wastewater

OPEN ACCESS

Edited by:
Xiaofei Tan,
Hunan University, China

Reviewed by:
Yongfu Guo,
Suzhou University of Science and Technology, China
Philiswa Nosizo Nomngongo,
University of Johannesburg, South Africa
Dingzhong Yuan,
East China University of Technology, China

****Correspondence:***
Rongjun Qu
rongjunqu@sohu.com

Specialty section:
This article was submitted to Sorption Technologies, a section of the journal Frontiers in Environmental Chemistry

Received: *07 May 2021*
Accepted: *30 August 2021*
Published: *01 November 2021*

Citation:
Xu T, Qu R, Zhang Y, Sun C, Wang Y, Kong X, Geng X and Ji C (2021) Amino-Thiol Bifunctional Polysilsesquioxane/Carbon Nanotubes Magnetic Composites as Adsorbents for Hg(II) Removal. Front. Environ. Chem. 2:706254. doi: 10.3389/fenvc.2021.706254

INTRODUCTION

Environmental problems caused by harmful pollutants have become serious threats to the survival of human beings and other living things (Hsu et al., 2021; Wang et al., 2021), and water pollution is particularly prominent among them. Common water pollutants include inorganic pollutants like heavy metal ions, acid, alkali and salt, and other organic pollutants (Mudasir et al., 2020, Wang et al., 2020a; Zhangal and Zhang, 2020) stem from metallurgy, chemical fiber, papermaking, printing and dyeing, and other industrial wastewaters (Khan et al., 2021; Verma and Balomajumder, 2020). Hg(II), Ni(II), Pb(II), and other heavy metal ions enter human body through the enrichment of the food chain and harm human health ultimately (Guo et al., 2020; Fu et al., 2021; Ge and Du, 2020), especially the strongest toxic mercury. Adsorption is more attractive in removing metal ions than chemical precipitation, sedimentation, ion exchange, filtration, and other traditional means (Zhao J. et al., 2018; Liu et al., 2019; Zhang B. et al., 2019), thanks to its simple operation, less secondary pollution, high adsorption efficiency, low cost, and other advantages (Zhao et al., 2012; Wang et al., 2017; Yang et al., 2019). Therefore, it is urgent to find a suitable adsorption material to treat Hg(II) in wastewater.

Carbon nanotubes (CNTs) are one novel nano-adsorbent used in water pollution treatment over the past decades (Alimohammady et al., 2017; Ahmadi et al., 2019). Compared to zeolite, kaolinite,

chitosan, biopolymer, and other traditional adsorption materials (Zhang M. et al., 2019; Fu et al., 2021; Khan et al., 2021), CNTs have more excellent aspect ratio, specific surface area, and unique one-dimensional structure (Sone et al., 2008; Zhao Y. et al., 2018; Aliyu, 2019), and all these structural features provide convenient conditions for metal ions adhering. Inevitably, the wide application of CNTs in adsorption field is also subjected to its own limitations (Basheer et al., 2020; Samareh and Siochi, 2017), such as poor dispersion, inferior dissolution, and skimp active sites. Hence, it has a great significance to modify CNTs with efficient functional molecules to maximize advantages in adsorption. Abbasi et al. (2021) prepared a novel calcined CuAl-layered double hydroxides/carbon nanotubes/polyvinylidene fluoride composites via a hydrothermal, casting, and calcination, and the composites show favorable adsorption properties to carminic acid. Alimohammady et al. (2017) reported a novel nano-adsorbent synthesized by the carboxylic multi-walled carbon nanotubes (MWCNTs-COOH) and 3-aminopyrazole, and the composite MWCNTs-f can remove 83.7% Cd(II) from aqueous solution at the optimum conditions. AlOmar et al. (2016) synthesized six deep eutectic solvents (DESs) systems based on choline chloride and six different hydrogen bond donors, and then the DESs were used to functionalize CNTs for adsorbing lead ions. Plentiful literatures indicating modified CNTs showed excellent adsorption performances in removing hazardous pollutants, include heavy metal ions, inorganic acid, and organics. Nonetheless, the exploration of modifying CNTs is still in progress, and researchers are working to find other substitutable molecules to prepared potential nano-adsorbents.

Polysilsesquioxane (PSQ) is a kind of organic-inorganic hybrid material with Si-O inorganic bond backbone and organic groups in side chains (El-Nahhalal et al., 2007; Kierys et al., 2018). Due to the special composition and structure, PSQ has many unique and excellent properties (Tang et al., 2013; Rathnayake et al., 2021), for instance, the organic groups connected with Si can be connected with other groups through different chemical reactions (Wang et al., 2014). In addition, PSQ has distinct corrosion resistance, thermal stability, chemical reactivity (Zhang D. et al., 2020; Liu et al., 2021), and can be used in semiconductor materials, catalysis, adsorption, and other fields (Wu et al., 2018; Park et al., 2020; Kong et al., 2021). PSQ as an adsorbent commonly has high adsorption capacity and adsorption rate (Sun et al., 2014; Wang et al., 2020b). Niu et al. (2014) prepared a thiol-functionalized PSQ used for adsorbing Hg(II) and Mn(II) from aqueous solution. Wang et al. (2017) prepared two types of fibrous adsorbents by coating thiol- and amino-functionalized PSQ on poly (*p*-phenylenetherephthal amide) fibers, and evaluated the adsorption properties of Hg(II).

In our previous work (Xu et al., 2021), the bifunctional PSQ/CNTs magnetic composites were prepared by sol-gel method with carboxylic carbon nanotubes (CNTs-COOH), 3-aminopropyl-trimethoxysilane (APTMS), and 3-mercaptopropyl-trimethoxysilane (MPTMS), at the same time, magnetic Fe_3O_4 was embedded into composites to improve the separation speed from aqueous solution (Yuan et al., 2016; Zhang S. et al., 2020). The composites were applied to recycle Au(III) from wastewater and the results indicated that the bifunctional PSQ/CNTs magnetic composites have excellent performances in adsorbing Au(III).

In the present work, we target investigating the adsorption abilities of the composites we prepared previously in treating low concentration Hg(II). Consequently, a complete set of adsorption experiments were operated and analyzed, mainly contain static adsorption, optimal pH, adsorption isotherms and kinetics, adsorption mechanism, selectivity, and recycle.

EXPERIMENTAL

Materials and Methods

All chemicals and reagents were of analytical grade and used as received unless otherwise stated. CNTs-COOH was purchased from Times nano, Chengdu Organic Chemicals Co., Ltd., China. APTMS was purchased from Shanghai Macklin Biochemical Co., Ltd., China. MPTMS was purchased from Qufu Wanda Chemical Co., Ltd., China. Mercuric nitrate ($Hg(NO_3)_2{\cdot}1/2H_2O$) were purchased from Sinopharm Chemical Reagent Co., Ltd., China.

Bifunctional PSQ/CNTs magnetic composites were synthesized by sol-gel method. The first step is magnetization; prepared magnetic Fe_3O_4 was embedded in the original material to give CNTs-COOH@Fe_3O_4, and then CNTs-COOH@Fe_3O_4 was coupled with APTMS via amidation to give the intermediate CNTs-APTMS@Fe_3O_4 with siloxane introduced on the surface. In the final step, CNTs-APTMS@Fe_3O_4 was decorated with variable proportions of APTMS and MPTMS to give the bifunctional PSQ/CNTs magnetic composites. The reaction steps as shown in **Figure 1** and the monofunctional PSQ/CNTs magnetic composites were also prepared in the same way for comparison. The specific experimental methods and dosages were described in Ref. Xu et al. (2021). The structures and surface morphologies of PSQ/CNTs magnetic composites were confirmed by FT-IR, SEM, VSM, XRD, XPS, and BET analysis, and all the characterization analyses were also detailed explicated in Ref. Xu et al. (2021).

Static Adsorption

For measuring the adsorption properties of the composites to different metal ions, 10 mg composite was added into 40 ml 100 mg L^{-1} $Hg(NO_3)_2{\cdot}1/2H_2O$, $AgNO_3$, $Pb(NO_3)_2$, $Cu(NO_3)_2{\cdot}3H_2O$, and $Ni(NO_3)_2{\cdot}6H_2O$, respectively. At the same time, the unmodified CNTs-COOH@Fe_3O_4 and the intermediate CNTs-APTMS@Fe_3O_4 were also measured in the same way. Then the mixtures were shaken at 25°C for 24 h. The initial and equilibrium concentrations of metal ions were measured by atomic absorption spectrometry (AAS). The adsorption capacity was calculated by the equation as follows:

$$q_e = \frac{(C_0 - C_e)V}{W} \quad (1)$$

where q_e (mmol g^{-1}) is the equilibrium adsorption capacity; C_0 and C_e (mmol L^{-1}) represent the initial and equilibrium concentration of metal ion, respectively; V (L) is the volume

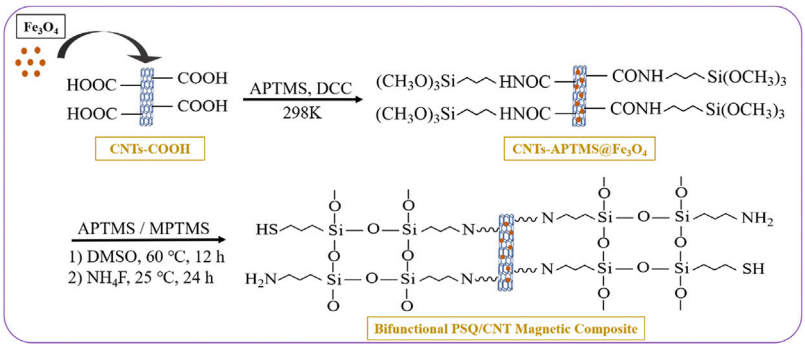

FIGURE 1 | Illustration for the synthesis of bifunctional PSQ/CNTs magnetic composites.

of solution; and W (g) is the weight of the composite adsorbent.

Optimal pH

The effect of pH on the uptake of composites for Hg(II) was performed by the following method: 10 mg composite was added into 40 ml 100 mg L^{-1} Hg(II) solution, the different solution pH values were adjusted with dilute HNO_3 and NaOH aqueous, after that the mixtures shaken at 25°C for 24 h. The initial and equilibrium concentrations were measured by AAS and the adsorption capacities were calculated by **Equation 1** as well.

Adsorption Isotherms

A total of 10 mg composite was added into 40 ml $Hg(NO_3)_2{\cdot}1/2H_2O$ solution with different initial concentrations, adjusted to optimal pH, and the mixtures were then shaken at 25°C for 24 h. Simultaneously, the same method was used to determine the adsorption capacities of the composites at 15 and 35°C and calculated with **Equation 1**.

Adsorption Kinetics

A total of 10 mg composite was added into 100 ml 50 mg L^{-1} Hg(II) solution, adjusted to optimal pH, and then shaken at 25°C. The concentrations of Hg(II) were determined at regular time intervals and calculated by the following equation as follows:

$$q_e = \frac{\sum (C_0 - C_t)V_t}{W} \quad (2)$$

where q_e (mmol g^{-1}) is the equilibrium adsorption capacity; C_0 and C_t (mmol L^{-1}) represent the initial and time t concentration of metal ion, respectively; V_t (L) is the volume of solution at time t; and W (g) is the weight of the composite adsorbent.

Adsorption Selectivity

A total of 10 mg composite was added into 40 ml solution with binary metal ions in the same concentrations (100 mg L^{-1}) and shaken at 25°C for 24 h. The concentrations of the two metal ions were determined by AAS, respectively, calculated with **Equation 1**,

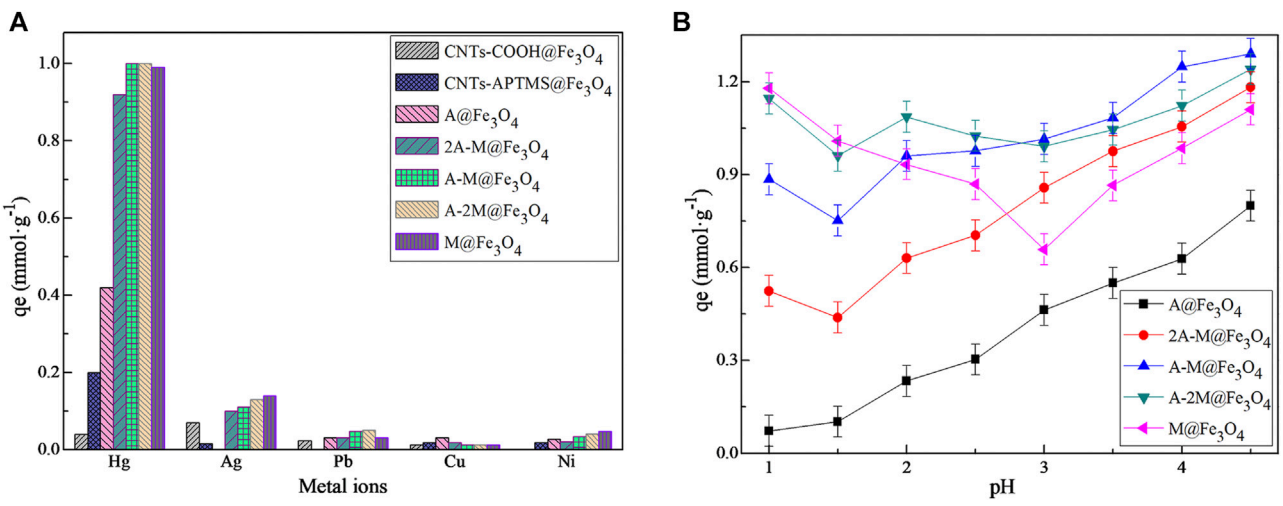

FIGURE 2 | (A) The static adsorption capacities of different materials for different metal ions at pH 2.5 and 25°C; **(B)** the effect of pH on different PSQ/CNTs magnetic composites adsorption for Hg(II).

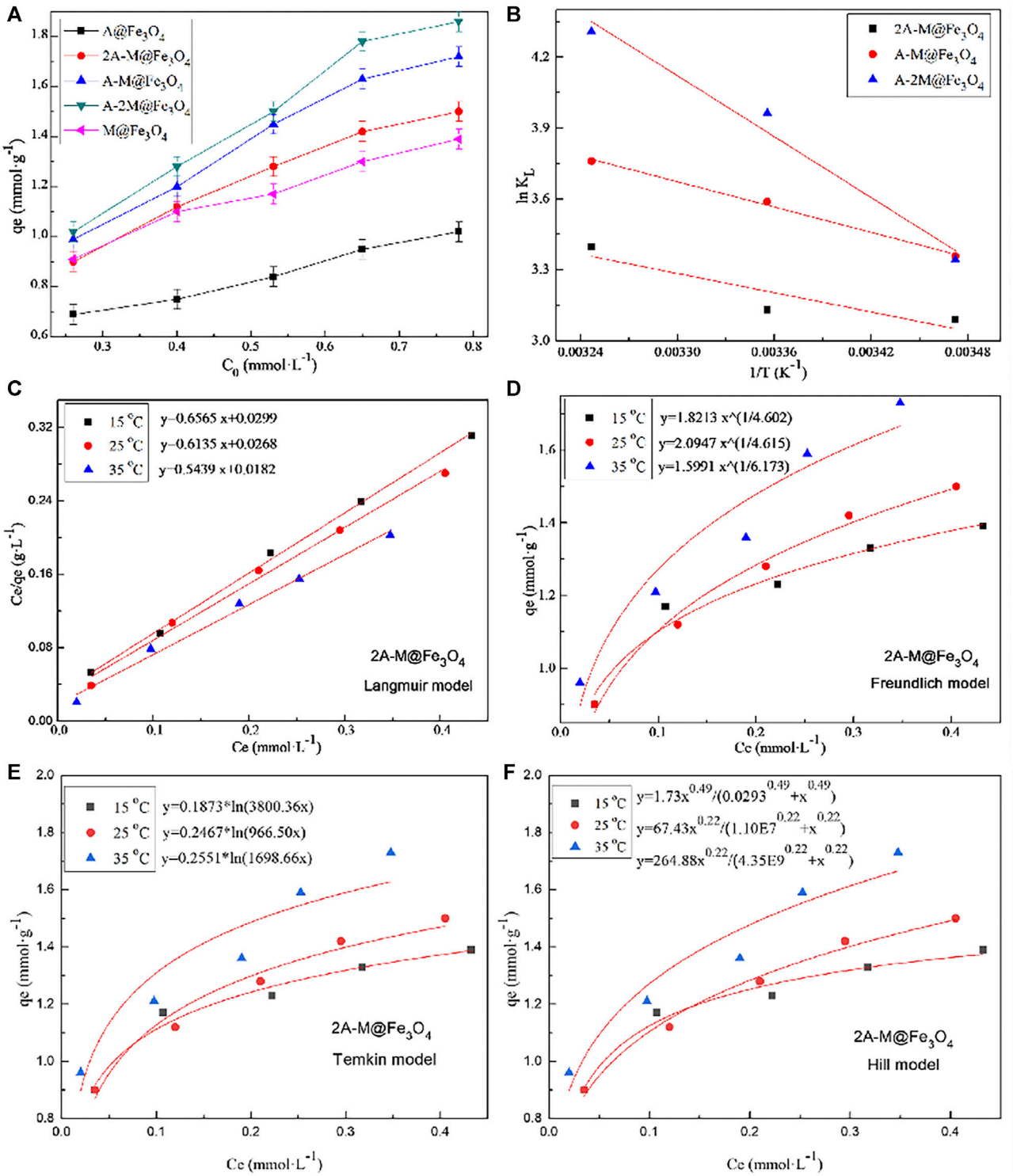

FIGURE 3 | (A) The adsorption capacities of composites for Hg(II) varies with initial concentration at pH 4.5 and 25°C; **(B)** the ln K_L~1/T lines of bifunctional composites for Hg(II); **(C)** Langmuir, **(D)** Freundlich, **(E)** Temkin, and **(F)** Hill fitting curves of 2A-M@Fe_3O_4 for Hg(II) at different temperatures.

TABLE 1 | Langmuir and Freundlich isotherm parameters of bifunctional PSQ/CNTs magnetic composites for Hg(II).

T (°C)	Adsorbents	Langmuir			Freundlich		
		q_{max} (mmol g^{-1})	K_L	R_L^2	K_F	n	R_F^2
15	2A-M@Fe_3O_4	1.52	21.95	0.9977	1.82	4.60	0.9878
	A-M@Fe_3O_4	1.52	28.75	0.9961	1.66	5.76	0.9347
	A-2M@Fe_3O_4	1.65	28.28	0.9838	1.73	6.00	0.8361
25	2A-M@Fe_3O_4	1.63	22.89	0.9902	2.09	4.61	0.9189
	A-M@Fe_3O_4	1.83	36.15	0.9918	2.04	5.48	0.8916
	A-2M@Fe_3O_4	1.94	52.63	0.9907	2.15	6.31	0.8336
35	2A-M@Fe_3O_4	1.84	29.88	0.9879	1.60	6.17	0.9581
	A-M@Fe_3O_4	1.91	42.97	0.9813	2.16	5.62	0.8247
	A-2M@Fe_3O_4	1.95	74.35	0.9901	2.44	4.98	0.9359

and then the adsorption selective coefficient (α) was defined as formula (3):

$$\alpha = \frac{\text{The adsorption capacity of Hg (II) on adsorbent}}{\text{The adsorption capacity of coexisting metal ion on adsorbent}} \quad (3)$$

Adsorption Mechanism

A total of 10 mg composite was added into the Hg(II) solution under the optimal conditions and shaken thermostatically for 24 h. It was filtered and then the adsorbent with metal ions anchored was placed in the oven at 60°C until completely dry. The mechanism of adsorption process was inferred by analyzing the changes of the elements in XPS spectra before and after adsorption.

Elution Regeneration

Different concentrations of eluents were prepared according to the acid environment that Hg(II) located. A total of 10 mg adsorbent with Hg(II) anchored was added into 40 ml eluent (0.1 mol L^{-1} HNO_3, 1, 2, 3, 4, and 5% thiourea in 0.1 mol L^{-1} HNO_3, respectively). It was then shaken at 25°C and desorption for 24 h, and the metal ion concentrations of eluents after desorption were measured by AAS, to determine the best eluent. Repeat adsorption-desorption three times, and judge the regeneration performances of the composites.

TABLE 3 | The adsorption thermodynamic parameters of bifunctional PSQ/CNTs magnetic composites for Hg(II) at different temperatures.

Adsorbents	T (K)	ΔG (kJ mol^{-1})	ΔH (kJ mol^{-1})	ΔS (J mol^{-1} K^{-1})
2A-M@Fe_3O_4	288	−7.305	11.276	64.518
	298	−7.950		
	308	−8.595		
A-M@Fe_3O_4	288	−8.055	14.836	79.482
	298	−8.850		
	308	−9.644		
A-2M@Fe_3O_4	288	−8.099	35.741	152.221
	298	−9.620		
	308	−11.143		

RESULTS AND DISCUSSION

Static Adsorption

The adsorption properties of different materials for metal ions are shown in **Figure 2A**. As you can see from the figure, the PSQ/CNTs magnetic composites showed excellent adsorption capacities for Hg(II) rather than Ag(I), Pb(II), Cu(II), and Ni(II). Compared with pristine CNTs-COOH@Fe_3O_4 and intermediate CNTs-APTMS@Fe_3O_4, PSQ/CNTs magnetic composites displayed more remarkable adsorption performance to Hg(II), and the adsorption capacities increased 0.3–0.9 mmol g^{-1} to different extent. Further, the bifunctional PSQ/CNTs magnetic composites expressed relatively higher adsorption capacities than monofunctional composites, especially the composite A@Fe_3O_4. As a whole, the bifunctional PSQ/CNTs magnetic composites showed superior adsorption abilities to Hg(II) and the systematic exploration would be further studied in the following.

Optimal pH

Figure 2B shows the effect of solution pH values on different composites for adsorbing Hg(II); the experimental pH values varied from 1.0 to 4.5. Obviously, the adsorption capacities of composites to Hg(II) were greatly affected by the solution pH values. To be specific, the monofunctional composite A@Fe_3O_4 showed consistent change with pH variation, and this can be interpreted as H^+ tends to compete with Hg^{2+} to form -NH_3^+ at relatively low pH values (Wang et al., 2017; Wang et al., 2019),

TABLE 2 | Temkin and Hill isotherm parameters of bifunctional PSQ/CNTs magnetic composites for Hg(II).

T (°C)	Adsorbents	Temkin			Hill			
		B_T	K_M	R_T^2	n_2	N_M	$C_{1/2}$	R_H^2
15	2A-M@Fe_3O_4	0.1873	3,800.36	0.9776	0.4941	3.50	0.0293	0.9591
	A-M@Fe_3O_4	0.1890	3,993.09	0.9203	0.1756	582.92	1.45E10	0.9015
	A-2M@Fe_3O_4	0.1839	6,985.38	0.8382	0.1679	964.03	5.19E11	0.7536
25	2A-M@Fe_3O_4	0.2467	966.50	0.9737	0.2212	304.84	1.10E7	0.9813
	A-M@Fe_3O_4	0.2158	5,805.33	0.8753	0.1834	1,337.62	2.13E11	0.8370
	A-2M@Fe_3O_4	0.1921	27,770.56	0.8260	0.1592	1,811.81	2.20E13	0.7500
35	2A-M@Fe_3O_4	0.2551	1,698.66	0.8986	0.2178	1,216.16	4.35E9	0.8779
	A-M@Fe_3O_4	0.2085	11,488.12	0.8112	0.1784	2,171.36	4.20E12	0.7367
	A-2M@Fe_3O_4	0.1403	1.10E6	0.8676	0.1119	1,376.14	4.47E16	0.8159

TABLE 4 | The adsorption capacity comparison of different adsorbents for Hg(II) at 25°C.

Adsorbents	Qe (mmol g^{-1})	References
GO functionalized by aminoethylpiperazine (AEP-GO)	0.54	Jin et al. (2020)
Tannic acid cross-linking cellulose/polythyleneimine composite (MCP)	1.24	Sun et al. (2021)
Cellulose nanofibrils (CNF)	0.66	Bisla et al. (2020)
Magnetic network polymer composite (MCTP)	1.22	Fu et al. (2021)
Bifunctional PSQ/fiber composite (PPTA-AM-70)	1.54	Wang et al. (2019)
2A-M@Fe_3O_4	1.63	This work
A-M@Fe_3O_4	1.83	This work
A-2M@Fe_3O_4	1.94	This work

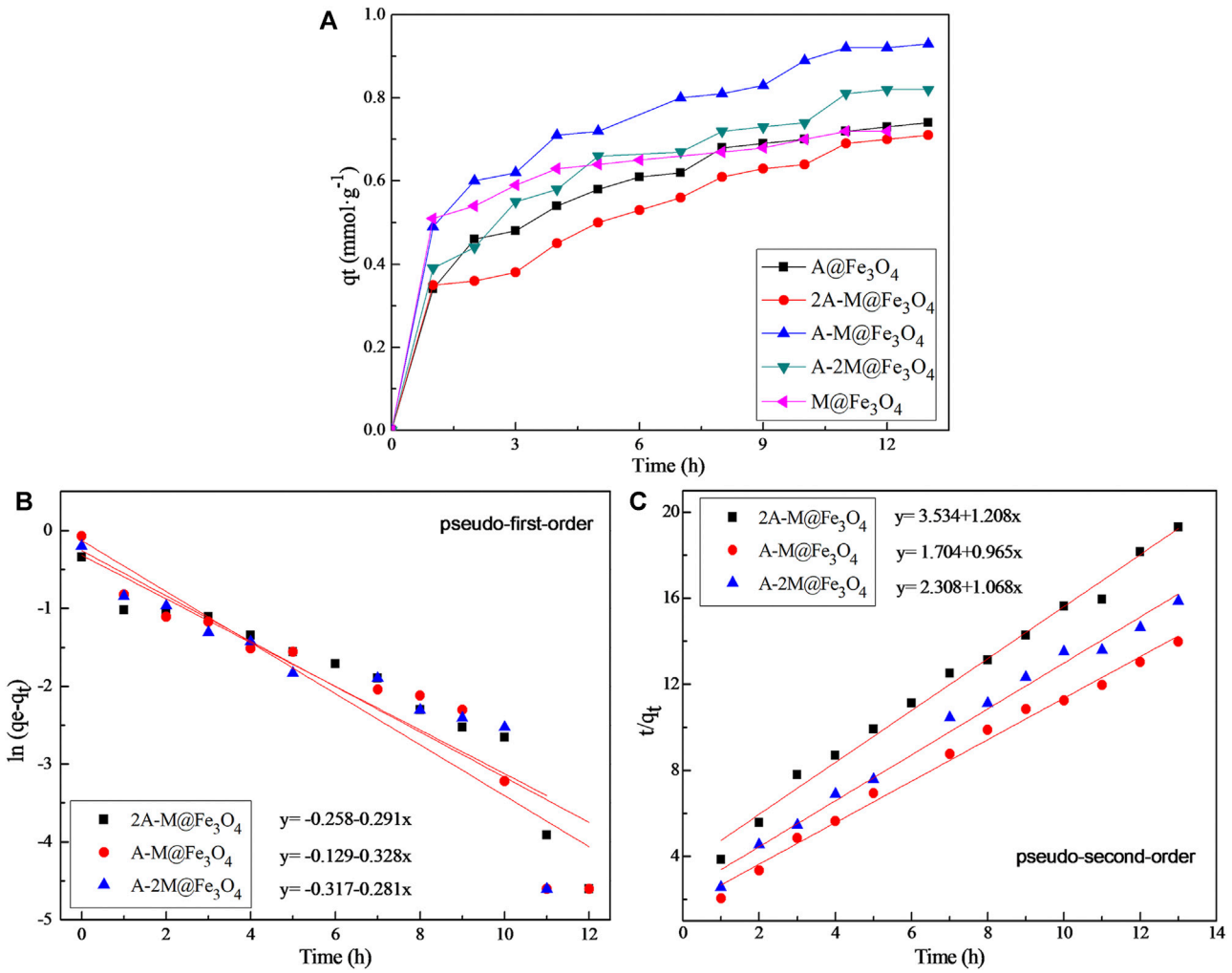

FIGURE 4 | (A) The adsorption kinetic curves of PSQ/CNTs magnetic composites for Hg(II) at pH 4.5 and 25°C; **(B)** the pseudo-first-order and **(C)** the pseudo-second-order adsorption models of bifunctional PSQ/CNTs magnetic composites for Hg(II).

the adsorbent surface is positively charged and electrostatic repulsion occurs with Hg^{2+}, thus the adsorption capacity is low at highly acidic solution. With the growth of pH value, the concentration of H^+ decreases and the protonation of -NH_2 weakens, and thus the adsorption amount of composite for Hg(II) increased spontaneously. For M@Fe_3O_4, the effect of solution pH was mainly divided into two parts, and the adsorption capacity reached the maximum at pH 4.5. For bifunctional composites, the adsorption capacities greatly affected by the thiol group before pH 1.5 and mainly affected by the amino group after pH 1.5, and finally reached the maximum at pH 4.5.

TABLE 5 | The adsorption kinetics parameters of bifunctional PSQ/CNTs magnetic composites for Hg(II) at 25°C.

Adsorbent	$Q_{e,\ exp}$ (mmol g^{-1})	Pseudo-first-order kinetics			Pseudo-second-order kinetics		
		K_1 (h^{-1})	$Q_{e,\ cal\ 1}$ (mmol g^{-1})	R_1^2	K_2 (g $mmol^{-1}$ h^{-1})	$Q_{e,\ cal\ 2}$ (mmol g^{-1})	R_2^2
2A-M@Fe_3O_4	0.710	0.291	0.773	0.8777	0.413	0.828	0.9882
A-M@Fe_3O_4	0.930	0.328	0.879	0.8740	0.547	1.036	0.9903
A-2M@Fe_3O_4	0.820	0.281	0.728	0.8097	0.495	0.936	0.9878

TABLE 6 | The adsorption selectivity of bifunctional PSQ/CNTs magnetic composites for Hg(II).

Adsorbents	System	Metal ions	q (mmol g^{-1})	Selectivity coefficient (α)
A-2M@Fe_3O_4	Hg (II) – Ag (I)	Hg (II)	1.08	9.8
		Ag (I)	0.11	
	Hg (II) – Pb (II)	Hg (II)	1.13	56.5
		Pb (II)	0.02	
	Hg (II) – Ni (II)	Hg (II)	1.06	∞
		Ni (II)	0.00	
	Hg (II) – Cu (II)	Hg (II)	1.03	∞
		Cu (II)	0.00	
	Hg (II) – Cd (II)	Hg (II)	1.05	∞
		Cd (II)	0.00	

Adsorption Isotherms

The adsorption isotherms of the composites for Hg(II) were carried out with initial concentration at 50, 75, 100, 125, and 150 mg L^{-1} at pH 4.5 and different temperatures. The adsorption capacities variation of PSQ/CNTs magnetic composites with initial concentration are shown in **Figure 3A**, and the bifunctional composites can basically achieve complete adsorption at relatively low initial concentrations; the monofunctional composites have less adsorption, especially the composite A@Fe_3O_4. As the initial concentrations increase, the equilibrium adsorption capacity of all composites increased.

The equilibrium adsorption isotherm plays an important part in investigating the adsorption mechanism and adsorption capacity (Li et al., 2019; Hu et al., 2021). Four types of adsorption model, Langmuir, Freundlich, Tempkin, and Hill models, were used to fit the adsorption process to further explore the thermodynamic adsorption for Hg(II). The Langmuir model deems that adsorption occurs on a monolayer of uniform surface with no interaction between the adsorbents (Zhao et al., 2019; Ghodsi et al., 2021); differently, the Freundlich mode deems that adsorption occurs on multilayers of heterogeneous surfaces. The Temkin model reflects that the reaction between the adsorbate and the adsorbent linearly reduces the heat of adsorption. The Hill model showed the relation of different species on the homogeneous surfaces and assumed that one adsorption site can capture n_2 ions. Where $n_2 > 1$ said positive cooperativity, $n_2 = 1$ proved non-cooperative and $n_2 < 1$ showed negative cooperativity between the binding (Saadi et al., 2015). The equations of the four models are as follows, respectively:

$$\frac{C_e}{q_e} = \frac{C_e}{q_{max}} + \frac{1}{q_{max} K_L} \tag{4}$$

$$q_e = K_F \cdot C_e^{\frac{1}{n}}, \tag{5}$$

$$q_e = B_T \cdot \ln(K_m C_e), \tag{6}$$

$$q_e = \frac{n_2 N_M C_e^{n_2}}{C_e^{n_2} + C_{1/2}^{n_2}} \tag{7}$$

where C_e (mmol L^{-1}) is the equilibrium solution concentration; q_e (mmol g^{-1}) is the equilibrium adsorption capacity; q_{max} (mmol g^{-1}) is the maximum adsorption capacity; K_L is the Langmuir constant; and K_F and n are the Freundlich constants related to adsorption capacity and strength, respectively. K_m was the constant of the Temkin model and B_T was related to the heat of adsorption. n_2, N_M, and $C_{1/2}$ were the number of the adsorbed ions at each site, the density of the receptor sites, and semi saturated concentration, respectively.

The fitting of the composite 2A-M@Fe_3O_4 at different temperatures to the four models are shown in **Figures 3C–F**, respectively, and the related parameters of all bifunctional PSQ/CNTs magnetic composites are calculated and shown in **Tables 1**, **2**. From the fitting curves in figure and parameters in the table, we can find that the fitted related coefficient $R_L^2 > R_F^2 > R_T^2 > R_H^2$, that is, the Langmuir model is more suitable to describe the thermodynamic process of composites to Hg(II) adsorption, and thus, the adsorption occurs on a monolayer with no interaction.

Further, thermodynamic parameters of the bifunctional PSQ/CNTs magnetic composites to Hg(II) were also calculated by **Equations 8**, **9**, including Gibbs free energy (ΔG), entropy change (ΔS), and enthalpy change (ΔH) (Niu et al., 2014):

$$\ln K_L = \frac{\Delta S}{R} - \frac{\Delta H}{RT} \tag{8}$$

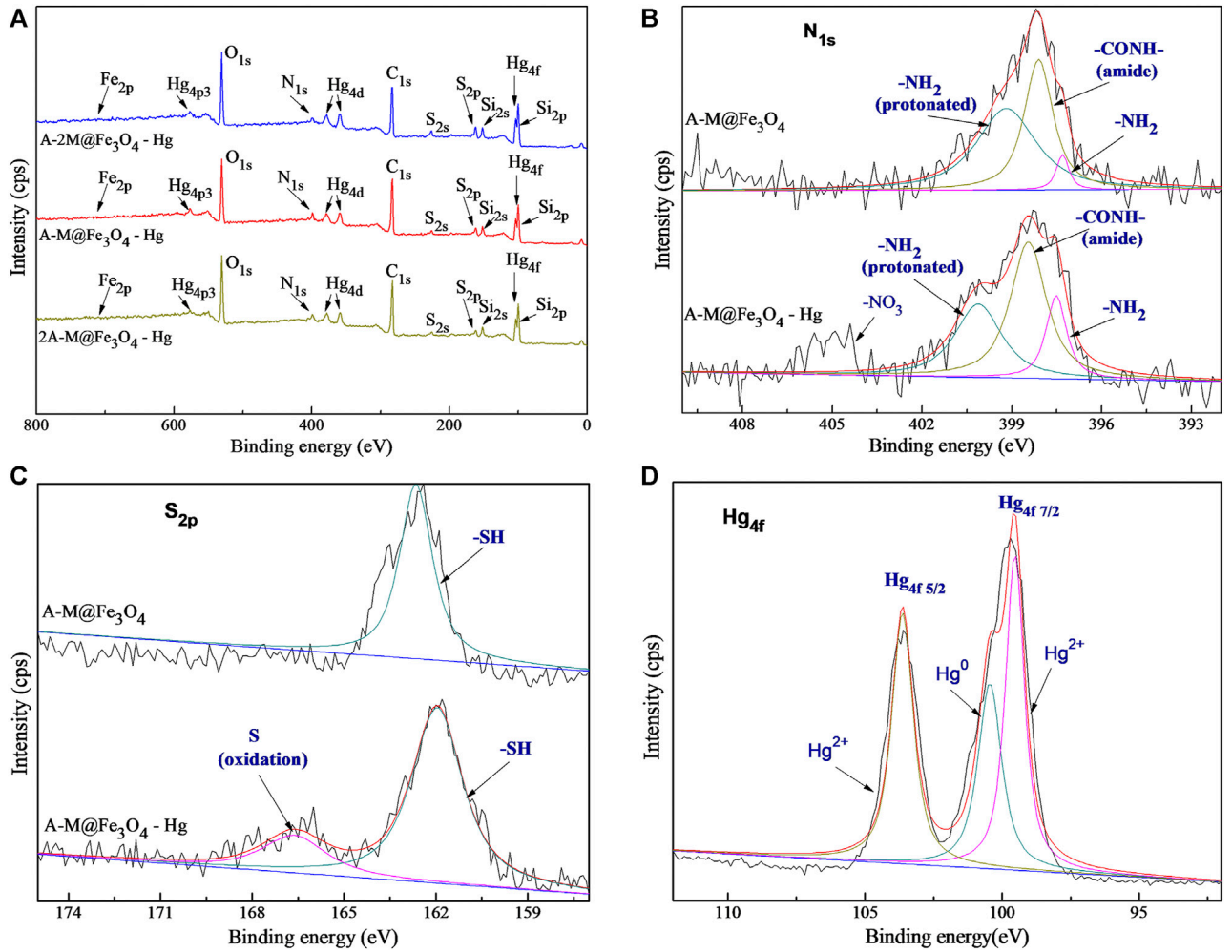

FIGURE 5 | (A) The wide scan XPS spectra of bifunctional PSQ/CNTs magnetic composites after Hg(II) adsorption; high-resolution XPS spectra of **(B)** N_{1s} and **(C)** S_{2p} of A-M@Fe_3O_4 before and after Hg(II) adsorption; **(D)** high-resolution XPS spectra of Hg_{4f}.

$$\Delta G = \Delta H - T\Delta S \quad (9)$$

where K_L is the Langmuir constant, R is the gas constant ($R = 8.314\ J\ mol^{-1}\ K^{-1}$), and T (K) is the experimental temperature.

Plotting ln K_L against $1/T$ to give fitting straight-lines of bifunctional PSQ/CNTs magnetic composites in **Figure 3B**, the slope and intercept are $-\Delta H/R$ and $\Delta S/R$, respectively. The adsorption thermodynamic parameters ΔG, ΔS, and ΔH were calculated in **Table 3**, in which the values are $\Delta G < 0$, $\Delta S > 0$, and $\Delta H > 0$, indicating that the adsorption process of bifunctional PSQ/CNTs magnetic composites to Hg(II) is a spontaneous, increased confusion and endothermic reaction process. That is to say, the whole adsorption process is a spontaneous behavior and we can promote the metal ions adhered on the surface of composites to enhance adsorption capacities by increasing temperatures. Compared with the adsorbents of the same type reported in the literature listed in **Table 4**, the adsorbents prepared in this paper show superior adsorption performance.

Adsorption Kinetics

Adsorption kinetics is a common method to characterize the adsorption efficiency and indicate the adsorption type of solute in the adsorption process (Yang et al., 2014; Wei et al., 2021). **Figure 4A** is the adsorption rate of all prepared PSQ/CNTs magnetic composites for Hg(II) at 25°C, and the adsorption rate fell in the following order: A-M@Fe_3O_4 > A-2M@Fe_3O_4 > M@Fe_3O_4 > A@Fe_3O_4 > 2A-M@Fe_3O_4. Obviously, the whole adsorption process for Hg(II) consists of two distinct parts, the first hour is the rapid adsorption stage to give the main adsorption capacity, the second stage is relatively smooth and slow to give the final equilibrium adsorption capacity. As can be seen from the figure, the adsorption process reached adsorption equilibrium in about 11–13 h.

For better exploring the adsorption process of PSQ/CNTs magnetic composites to Hg(II), the kinetics data were fitted into

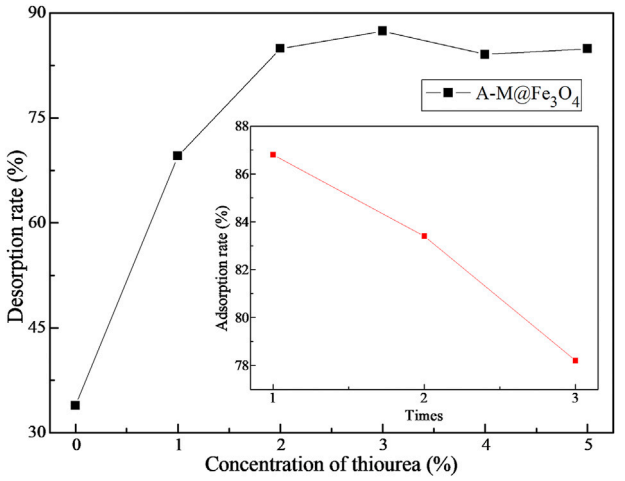

FIGURE 6 | The effect of thiourea concentration on the desorption rate of Hg(II) and the elution regeneration adsorption rate of A-M@Fe_3O_4 (inset).

the pseudo-first-order and pseudo-second-order models (Wang et al., 2019; Wang L. et al., 2020) as follows, respectively:

$$\ln(q_e - q_t) = \ln q_e - k_1 t \quad (10)$$

$$\frac{t}{q_t} = \frac{1}{k_2 q_e^2} + \frac{t}{q_e} \quad (11)$$

where q_e and q_t (mmol g^{-1}) are the adsorption capacity for Hg(II) at equilibrium and time t (h), respectively; k_1 (h^{-1}) and k_2 (g $mmol^{-1}h^{-1}$) are the rate constant of pseudo-first-order and pseudo-second-order models.

Figures 4B,C and **Table 5** show the fitting results and the specific kinetic parameters of bifunctional PSQ/CNTs magnetic composites to the two models. As can be seen from the fitting lines and data, the pseudo-second-order model has higher correlation coefficient than the pseudo-first-order model ($R_2^2 > R_1^2$). That is, the pseudo-second-order model is more suitable to describe the adsorption process for Hg(II), thus, the limiting step of adsorption rate may be chemical adsorption involving valency forces through the sharing or exchange of electrons between PSQ/CNTs and Hg(II) (Qu et al., 2009).

Adsorption Selectivity

The adsorption selectivity is an important factor to evaluate the adsorption properties of adsorbents (Mudasir et al., 2020; Wang et al., 2020a), thus, the adsorption selectivity of the representative composite A-2M@Fe_3O_4 for Hg(II) with common coexisting metal ions was carried out. The experiments were operated at optimal pH (pH = 4.5) and the results in **Table 6** suggested that the composite tend to adsorb Hg(II) rather than coexisting metal ions, especially ions Pb(II), Ni(II), Cu(II), and Cd(II). The selectivity coefficient is relatively low when Ag(I) coexists with Hg(II), and this can be interpreted by the hard-soft acid-base theory (HSAB). Hg(II) and Ag(I) are classified as soft ions and can form high affinity with functional groups containing nitrogen and sulfur, thus the coexistence of Ag(I) has a great influence on the adsorption of Hg(II). As a whole, the bifunctional PSQ/CNTs magnetic composites can potentially adsorb and separate Hg(II) in coexisting metal ions system.

Adsorption Mechanism

The binding energy changes of elements in XPS scan before and after adsorption were analyzed to infer the adsorption mechanism for Hg(II). **Figure 5A** shows the wide scan XPS spectra of bifunctional PSQ/CNTs magnetic composites after Hg(II) adsorption, the binding energy peaks of Hg_{4f} and Hg_{4d} are clearly displayed in the curves, and the peak of Hg_{4p} is easily found as well. The binding energy peaks of Hg_{4f} at 99.8 and 103.6 eV in **Figure 5D** are vested to $Hg_{4f\ 5/2}$ and $Hg_{4f\ 7/2}$ (Guo et al., 2020; Xia et al., 2021), respectively. Further, the main high-resolution peaks of $Hg_{4f\ 7/2}$ contains two different valence state peaks Hg^{2+} and Hg^0 (Wang et al., 2020b), which located at 99.6 and 100.5 eV, respectively, indicating that the redox reaction may occur in the process of adsorbing Hg(II). The element binding energy changes of the composite A-M@Fe_3O_4 before and after adsorption are displayed in **Figures 5B,C**. In the spectra of N_{1s}, the binding energy shifts from 397.3 to 397.5 eV for -NH_2 and the relative peak area increased, the binding energy shifts from 398.1 to 398.4 eV for -CONH-, the binding energy shifts from 399.2 to 400.1 eV for the protonated -NH_3^+. The changes of binding energy and peak area indicate that chelation or ion exchange may occur during the process of adsorbing Hg(II). Similarly, in the spectra of S_{2p}, the binding energy of -SH shifts from 162.6 to 161.8 eV, indicating that chelation or ion exchange may be carried out. Meanwhile, the binding energy of oxidized S appeared at around 166.5 eV, which can be inferred that redox reaction may took place between -SH and Hg(II), and corresponds to the reduction of Hg^{2+}. In short, chelation or ion exchange may primarily occurred in the whole adsorption process, and certainly, limited redox reaction took place as well.

Elution Regeneration

The composite A-M@Fe_3O_4 was selected to explore the elution and regeneration performance for Hg(II), the desorption rate of A-M@Fe_3O_4 in a series of 0.1 mol L^{-1} HCl solution with different concentrations of thiourea eluents shown in **Figure 6**. Obviously, the desorption rate reached maximum in 0.1 mol L^{-1} HCl solution with 3% thiourea eluents; thus, the following elution experiments were taking place in it and the adsorption rate varied with regeneration times shown in **Figure 6** inset. The adsorption rate gradually decreased with the increasing of regeneration frequency and the adsorption rate still achieved 78% after repeat elution-regeneration three times. That is to say, the bifunctional PSQ/CNTs magnetic composites have favorable regenerability and can be expected to be a kind of potential economic adsorbent.

CONCLUSION

Amino-thiol bifunctional PSQ/CNTs magnetic composites were successfully prepared by amidation and condensation between CNTs and two types of siloxane. The systematic adsorption experiments showed that the composites have favorable adsorption properties for low concentration Hg(II) removal. Specifically, the static adsorption indicates that the bifunctional PSQ/CNTs magnetic composites have superior adsorption capacities than monofunctional composites, pristine material CNTs-COOH@Fe_3O_4, and common intermediate CNTs-APTMS@Fe_3O_4, particularly, the adsorption capacities increase 0.3–0.9 mmol g^{-1} to different extent compared to unfunctional materials. The thermodynamic curves are more consistent with the Langmuir model and the kinetics curves are fitted to the pseudo-second-order model well. The maximal adsorption capacities of the bifunctional composites for Hg(II) varied from 1.63 to 1.94 mmol g^{-1} at 25°C according to the Langmuir model, and the kinetics indicate that the rate-determining step of the adsorption process may be controlled by chemical reactions. Selectivity experiments declare that the composites tend to adsorb Hg(II) rather than a bunch of other coexisting metal ions and the adsorption rate could still reach 78% after repeating the cycle three times in elution regeneration tests. Although the adsorption capacity is a little lower compared to Au(III), the bifunctional PSQ/CNTs magnetic composite is still anticipated to be an adsorbent with potential practical value in adsorbing low concentration harmful metal ions Hg(II) from waste water.

DATA AVAILABILITY STATEMENT

The original contributions presented in the study are included in the article/**Supplementary Material**, further inquiries can be directed to the corresponding author.

AUTHOR CONTRIBUTIONS

TX: writer, main contributor RQ: corresponding author, supervisor YZ, CS, YW, XK, XG, and CJ: data contributors.

FUNDING

This study was funded by the National Natural Science Foundation of China (52073135, 51673089, 51903114), Yantai Research Institute for the Transformation of Old and New Kinetic Forces (2019XJDN001), and Natural Science Foundation of Shandong Province (ZR2020ME066).

SUPPLEMENTARY MATERIAL

The Supplementary Material for this article can be found online at: https://www.frontiersin.org/articles/10.3389/fenvc.2021.706254/full#supplementary-material

REFERENCES

Abbasi, M., Sabzehmeidani, M. M., Ghaedi, M., Jannesar, R., and Shokrollahi, A. (2021). Adsorption Performance of Calcined Copper-Aluminum Layered Double hydroxides/CNT/PVDF Composite Films toward Removal of Carminic Acid. *J. Mol. Liquids* 329, 115558. doi:10.1016/j.molliq.2021.115558

Ahmadi, S., Igwegbe, C. A., Rahdar, S., and Asadi, Z. (2019). The Survey of Application of the Linear and Nonlinear Kinetic Models for the Adsorption of Nickel(II) by Modified Multi-Walled Carbon Nanotubes. *Appl. Water Sci.* 9. doi:10.1007/s13201-019-0978-9

Alimohammady, M., Jahangiri, M., Kiani, F., and Tahermansouri, H. (2017). A New Modified MWCNTs with 3-aminopyrazole as a Nanoadsorbent for Cd(II) Removal from Aqueous Solutions. *J. Environ. Chem. Eng.* 5, 3405–3417. doi:10.1016/j.jece.2017.06.045

Aliyu, A. (2019). Synthesis, Electron Microscopy Properties and Adsorption Studies of Zinc (II) Ions (Zn2+) onto As-Prepared Carbon Nanotubes (CNTs) Using Box-Behnken Design (BBD). *Scientific Afr.* 3, e00069. doi:10.1016/j.sciaf.2019.e00069

AlOmar, M. K., Alsaadi, M. A., Hayyan, M., Akib, S., Ibrahim, R. K., and Hashim, M. A. (2016). Lead Removal from Water by Choline Chloride Based Deep Eutectic Solvents Functionalized Carbon Nanotubes. *J. Mol. Liquids* 222, 883–894. doi:10.1016/j.molliq.2016.07.074

Basheer, B. V., George, J. J., Siengchin, S., and Parameswaranpillai, J. (2020). Polymer Grafted Carbon Nanotubes-Synthesis, Properties, and Applications: A Review. *Nano-Structures & Nano-Objects* 22, 100429. doi:10.1016/j.nanoso.2020.100429

Bisla, V., Rattan, G., Singhal, S., and Kaushik, A. (2020). Green and Novel Adsorbent from rice Straw Extracted Cellulose for Efficient Adsorption of Hg (II) Ions in an Aqueous Medium. *Int. J. Biol. Macromolecules* 161, 194–203. doi:10.1016/j.ijbiomac.2020.06.035

El-Nahhal, I. M., and El-Ashgar, N. M. (2007). A Review on Polysiloxane-Immobilized Ligand Systems: Synthesis, Characterization and Applications. *J. Organomet. Chem.* 692, 2861–2886. doi:10.1016/j.jorganchem.2007.03.009

Fu, Y., Sun, Y., Zheng, Y., Jiang, J., Yang, C., Wang, J., et al. (2021). New Network Polymer Functionalized Magnetic-Mesoporous Nanoparticle for Rapid Adsorption of Hg(II) and Sequential Efficient Reutilization as a Catalyst. *Separation Purif. Technology* 259, 118112. doi:10.1016/j.seppur.2020.118112

Ge, H., and Du, J. (2020). Selective Adsorption of Pb(II) and Hg(II) on Melamine-Grafted Chitosan. *Int. J. Biol. Macromolecules* 162, 1880–1887. doi:10.1016/j.ijbiomac.2020.08.070

Ghodsi, S., Behbahani, M., Yegane Badi, M., Ghambarian, M., Sobhi, H. R., and Esrafili, A. (2021). A New Dendrimer-Functionalized Magnetic Nanosorbent for the Efficient Adsorption and Subsequent Trace Measurement of Hg (II) Ions in Wastewater Samples. *J. Mol. Liquids* 323, 114472. doi:10.1016/j.molliq.2020.114472

Guo, Z., Kang, Y., Liang, S., and Zhang, J. (2020). Detection of Hg(II) in Adsorption experiment by a Lateral Flow Biosensor Based on Streptavidin-Biotinylated DNA Probes Modified Gold Nanoparticles and Smartphone Reader. *Environ. Pollut.* 266, 115389. doi:10.1016/j.envpol.2020.115389

Hsu, C.-J., Xiao, Y.-Z., and Hsi, H.-C. (2021). Simultaneous Aqueous Hg(II) Adsorption and Gaseous Hg0 Re-emission Inhibition from SFGD Wastewater by Using Cu and S Co-impregnated Activated Carbon. *Chemosphere* 263, 127966. doi:10.1016/j.chemosphere.2020.127966

Hu, X., Chen, C., Zhang, D., and Xue, Y. (2021). Kinetics, Isotherm and Chemical Speciation Analysis of Hg(II) Adsorption over Oxygen-Containing MXene Adsorbent. *Chemosphere* 278, 130206. doi:10.1016/j.chemosphere.2021.130206

Jin, J.-U., Yeo, H., Hahn, J. R., Yu, J., Ku, B.-C., and You, N.-H. (2020). Multifunctional Aminoethylpiperazine-Modified Graphene Oxide with High Dispersion Stability in Polar Solvents for Mercury Ion Adsorption. *J. Ind. Eng. Chem.* 90, 224–231. doi:10.1016/j.jiec.2020.07.015

Khan, F. S. A., Mubarak, N. M., Tan, Y. H., Khalid, M., Karri, R. R., Walvekar, R., et al. (2021). A Comprehensive Review on Magnetic Carbon Nanotubes and

Carbon Nanotube-Based Buckypaper for Removal of Heavy Metals and Dyes. *J. Hazard. Mater.* 413, 125375. doi:10.1016/j.jhazmat.2021.125375

Kierys, A., Borowski, P., Zaleski, R., and Barczak, M. (2018). Formation of Polysilsesquioxane Network by Vapor-phase Method in the Spatially Limited System of Cross-Linked Polymer Pores. *Polymer* 141, 202–212. doi:10.1016/j.polymer.2018.03.013

Kong, Q., Li, Z., Ding, F., and Ren, X. (2021). Hydrophobic N-Halamine Based POSS Block Copolymer Porous Films with Antibacterial and Resistance of Bacterial Adsorption Performances. *Chem. Eng. J.* 410, 128407. doi:10.1016/j.cej.2021.128407

Li, L., Bi, R., Wang, Z., Xu, C., Li, B., Luan, L., et al. (2019). Speciation of Mercury Using High-Performance Liquid Chromatography-Inductively Coupled Plasma Mass Spectrometry Following Enrichment by Dithizone Functionalized Magnetite-Reduced Graphene Oxide. *Spectrochimica Acta B: At. Spectrosc.* 159, 105653. doi:10.1016/j.sab.2019.105653

Liu, F., Peng, G., Li, T., Yu, G., and Deng, S. (2019). Au(III) Adsorption and Reduction to Gold Particles on Cost-Effective Tannin Acid Immobilized Dialdehyde Corn Starch. *Chem. Eng. J.* 370, 228–236. doi:10.1016/j.cej.2019.03.208

Liu, S., Guo, R., Li, C., Lu, C., Yang, G., Wang, F., et al. (2021). POSS Hybrid Hydrogels: A Brief Review of Synthesis, Properties and Applications. *Eur. Polym. J.* 143, 110180. doi:10.1016/j.eurpolymj.2020.110180

Mudasir, M., Baskara, R. A., Suratman, A., Yunita, K. S., Perdana, R., and Puspitasari, W. (2020). Simultaneous Adsorption of Zn(II) and Hg(II) Ions on Selective Adsorbent of Dithizone-Immobilized Bentonite in the Presence of Mg(II) Ion. *J. Environ. Chem. Eng.* 8, 104002. doi:10.1016/j.jece.2020.104002

Niu, Y., Qu, R., Liu, X., Mu, L., Bu, B., Sun, Y., et al. (2014). Thiol-functionalized Polysilsesquioxane as Efficient Adsorbent for Adsorption of Hg(II) and Mn(II) from Aqueous Solution. *Mater. Res. Bull.* 52, 134–142. doi:10.1016/j.materresbull.2014.01.024

Park, S., Kim, J.-Y., Choi, W., Lee, M.-J., Heo, J., Choi, D., et al. (2020). Ladder-like Polysilsesquioxanes with Antibacterial Chains and Durable Siloxane Networks. *Chem. Eng. J.* 393, 124686. doi:10.1016/j.cej.2020.124686

Qu, R., Sun, C., Wang, M., Ji, C., Xu, Q., Zhang, Y., et al. (2009). Adsorption of Au(III) from Aqueous Solution Using Cotton Fiber/chitosan Composite Adsorbents. *Hydrometallurgy* 100, 65–71. doi:10.1016/j.hydromet.2009.10.008

Rathnayake, H., White, J., and Dawood, S. (2021). Polysilsesquioxane-based Organic-Inorganic Hybrid Nanomaterials and Their Applications towards Organic Photovoltaics. *Synth. Met.* 273, 116705. doi:10.1016/j.synthmet.2021.116705

Saadi, R., Saadi, Z., Fazaeli, R., and Fard, N. E. (2015). Monolayer and Multilayer Adsorption Isotherm Models for Sorption from Aqueous media. *Korean J. Chem. Eng.* 32, 787–799. doi:10.1007/s11814-015-0053-7

Samareh, J. A., and Siochi, E. J. (2017). Systems Analysis of Carbon Nanotubes: Opportunities and Challenges for Space Applications. *Nanotechnology* 28, 372001. doi:10.1088/1361-6528/aa7c5a

Sone, H., Fugetsu, B., Tsukada, T., and Endo, M. (2008). Affinity-based Elimination of Aromatic VOCs by Highly Crystalline Multi-Walled Carbon Nanotubes. *Talanta* 74, 1265–1270. doi:10.1016/j.talanta.2007.08.041

Sun, C., Li, C., Qu, R., Zhang, Y., Bingdong, Z., and Kuang, Y. (2014). Syntheses of Diethylenetriamine-Bridged Polysilsesquioxanes and Their Structure-Adsorption Properties for Hg(II) and Ag(I). *Chem. Eng. J.* 240, 369–378. doi:10.1016/j.cej.2013.11.092

Sun, Y., Wu, Y., Fu, Y., Yang, C. Y., Jiang, J. W., Yan, G. Y., et al. (2021). Rapid and High Selective Removal of Hg(II) Ions Using Tannic Acid Cross-Linking Cellulose/polyethyleneimine Functionalized Magnetic Composite. *Int. J. Biol. Macromol.* 182, 1120. doi:10.1016/j.ijbiomac.2021.04.091

Tang, Y., Gou, J., and Hu, Y. (2013). Covalent Functionalization of Carbon Nanotubes with Polyhedral Oligomeric Silsequioxane for Superhydrophobicity and Flame Retardancy. *Polym. Eng. Sci.* 53, 1021–1030. doi:10.1002/pen.23338

Verma, B., and Balomajumder, C. (2020). Surface Modification of One-Dimensional Carbon Nanotubes: A Review for the Management of Heavy Metals in Wastewater. *Environ. Technology Innovation* 17, 100596. doi:10.1016/j.eti.2019.100596

Wang, C., Lin, G., Xi, Y., Li, X., Huang, Z., Wang, S., et al. (2020a). Development of Mercaptosuccinic Anchored MOF through One-step Preparation to Enhance Adsorption Capacity and Selectivity for Hg(II) and Pb(II). *J. Mol. Liquids* 317, 113896. doi:10.1016/j.molliq.2020.113896

Wang, C., Lin, G., Zhao, J., Wang, S., and Zhang, L. (2020b). Enhancing Au(III) Adsorption Capacity and Selectivity via Engineering MOF with Mercapto-1,3,4-Thiadiazole. *Chem. Eng. J.* 388, 124221. doi:10.1016/j.cej.2020.124221

Wang, L., Xu, H., Qiu, Y., Liu, X., Huang, W., Yan, N., et al. (2020). Utilization of Ag Nanoparticles Anchored in Covalent Organic Frameworks for Mercury Removal from Acidic Waste Water. *J. Hazard. Mater.* 389, 121824. doi:10.1016/j.jhazmat.2019.121824

Wang, W., Chen, M., Chen, X., and Wang, J. (2014). Thiol-rich Polyhedral Oligomeric Silsesquioxane as a Novel Adsorbent for Mercury Adsorption and Speciation. *Chem. Eng. J.* 242, 62–68. doi:10.1016/j.cej.2013.12.063

Wang, Y., Bao, S., Liu, Y., Yu, Y., Yang, W., Xu, S., et al. (2021). CoS2/GO Nanocomposites for Highly Efficient and Ppb Level Adsorption of Hg(II) from Wastewater. *J. Mol. Liquids* 322, 114899. doi:10.1016/j.molliq.2020.114899

Wang, Y., Qu, R., Mu, Y., Sun, C., Ji, C., Zhang, Y., et al. (2019). Amino- and Thiol-Polysilsesquioxane Simultaneously Coating on Poly(p-Phenylenetherephthal Amide) Fibers: Bifunctional Adsorbents for Hg(II). *Front. Chem.* 7, 465. doi:10.3389/fchem.2019.00465

Wang, Y., Qu, R., Pan, F., Jia, X., Sun, C., Ji, C., et al. (2017). Preparation and Characterization of Thiol- and Amino-Functionalized Polysilsesquioxane Coated Poly (P -phenylenetherephthal Amide) Fibers and Their Adsorption Properties towards Hg(II). *Chem. Eng. J.* 317, 187–203. doi:10.1016/j.cej.2017.02.073

Wei, Z., Zhang, Y., Ma, X., and Wang, W. (2021). Insight into the High-Efficiency Adsorption of Pyrene by Schiff Base Porous Polymers: Modelling and Mechanism. *Polymer* 220, 123576. doi:10.1016/j.polymer.2021.123576

Wu, Z., Cheng, X., Zhang, L., Li, J., and Yang, C. (2018). Sol-gel Synthesis of Preceramic Polyphenylsilsesquioxane Aerogels and Their Application toward Monolithic Porous SiOC Ceramics. *Ceramics Int.* 44, 14947–14951. doi:10.1016/j.ceramint.2018.05.115

Xia, J., Wang, Q., Yang, M., and Wu, H. (2021). Reliable Electroanalysis of Hg(II) in Water via Flower-like Porous MnCo2O4: Excellent Multilayer Adsorption and (Mn, Co)(II)/(Mn, Co)(III) Cycles. *Sensors Actuators B: Chem.* 326, 129008. doi:10.1016/j.snb.2020.129008

Xu, T., Qu, R., Zhang, Y., Sun, C., Wang, Y., Kong, X., et al. (2021). Preparation of Bifunctional Polysilsesquioxane/carbon Nanotube Magnetic Composites and Their Adsorption Properties for Au (III). *Chem. Eng. J.* 410, 128225. doi:10.1016/j.cej.2020.128225

Yang, H., Zhang, J., Liu, Y., Wang, L., Bai, L., Yang, L., et al. (2019). Rapid Removal of Anionic Dye from Water by Poly(ionic Liquid)-Modified Magnetic Nanoparticles. *J. Mol. Liquids* 284, 383–392. doi:10.1016/j.molliq.2019.04.029

Yang, R., Aubrecht, K. B., Ma, H., Wang, R., Grubbs, R. B., Hsiao, B. S., et al. (2014). Thiol-modified Cellulose Nanofibrous Composite Membranes for Chromium (VI) and lead (II) Adsorption. *Polymer* 55, 1167–1176. doi:10.1016/j.polymer.2014.01.043

Yuan, D., Chen, L., Xiong, X., Yuan, L., Liao, S., and Wang, Y. (2016). Removal of Uranium (VI) from Aqueous Solution by Amidoxime Functionalized Superparamagnetic Polymer Microspheres Prepared by a Controlled Radical Polymerization in the Presence of DPE. *Chem. Eng. J.* 285, 358–367. doi:10.1016/j.cej.2015.10.014

Zhang, B., Niu, Y., Li, L., Xu, W., Chen, H., Yuan, B., et al. (2019). Combined Experimental and DFT Study on the Adsorption of Co(II) and Zn(II) from Fuel Ethanol by Schiff Base Decorated Magnetic Fe3O4 Composites. *Microchemical J.* 151, 104220. doi:10.1016/j.microc.2019.104220

Zhang, D., Yi, J., Zhong, B., Ma, W., Peng, X., and Yang, D. (2020). A green Approach for Tunable Fluorescent and Superhydrophobic Monodisperse Polysilsesquioxane Spheres. *J. Colloid Interf. Sci.* 578, 484–490. doi:10.1016/j.jcis.2020.06.021

Zhang, H., and Zhang, J. (2020). The Preparation of Novel Polyvinyl Alcohol (PVA)-based Nanoparticle/carbon Nanotubes (PNP/CNTs) Aerogel for Solvents Adsorption Application. *J. Colloid Interf. Sci.* 569, 254–266. doi:10.1016/j.jcis.2020.02.053

Zhang, M., Zhang, S., Liu, X., Chen, H., Ming, Y., Xu, Q., et al. (2019). One-pot Synthesis of Multi-Functional and Environmental Friendly Tannic Acid Polymer with Fe3+ and Formaldehyde as Double Crosslinking Agents for

Selective Removal of Cation Pollutants. *Environ. Sci. Pollut. Res.* 26, 31834–31845. doi:10.1007/s11356-019-06297-2

Zhang, S., Yuan, D., Zhang, Q., Wang, Y., Liu, Y., Zhao, J., et al. (2020). Highly Efficient Removal of Uranium from Highly Acidic media Achieved Using a Phosphine Oxide and Amino Functionalized Superparamagnetic Composite Polymer Adsorbent. *J. Mater. Chem. A.* 8, 10925–10934. doi:10.1039/d0ta01633k

Zhao, B., Song, J., Fang, T., Liu, P., Jiao, Z., Zhang, H., et al. (2012). Hydrothermal Method to Prepare Porous NiO Nanosheet. *Mater. Lett.* 67, 24–27. doi:10.1016/j.matlet.2011.09.057

Zhao, J., Niu, Y., Ren, B., Chen, H., Zhang, S., Jin, J., et al. (2018). Synthesis of Schiff Base Functionalized Superparamagnetic Fe3O4 Composites for Effective Removal of Pb(II) and Cd(II) from Aqueous Solution. *Chem. Eng. J.* 347, 574–584. doi:10.1016/j.cej.2018.04.151

Zhao, J., Wang, C., Wang, S., Zhang, L., and Zhang, B. (2019). Selective Recovery of Au(III) from Wastewater by a Recyclable Magnetic Ni0.6Fe2.4O4 Nanoparticels with Mercaptothiadiazole: Interaction Models and Adsorption Mechanisms. *J. Clean. Prod.* 236, 117605. doi:10.1016/j.jclepro.2019.117605

Zhao Y., Y., Qin, J., Xu, H., Gao, S., Jiang, T., Zhang, S., et al. (2018). Gold Nanorods Decorated with Graphene Oxide and Multi-Walled Carbon Nanotubes for Trace Level Voltammetric Determination of Ascorbic Acid. *Microchim Acta* 186, 17. doi:10.1007/s00604-018-3138-2

Conflict of Interest: The authors declare that the research was conducted in the absence of any commercial or financial relationships that could be construed as a potential conflict of interest.

Publisher's Note: All claims expressed in this article are solely those of the authors and do not necessarily represent those of their affiliated organizations, or those of the publisher, the editors and the reviewers. Any product that may be evaluated in this article, or claim that may be made by its manufacturer, is not guaranteed or endorsed by the publisher.

Copyright © 2021 Xu, Qu, Zhang, Sun, Wang, Kong, Geng and Ji. This is an open-access article distributed under the terms of the Creative Commons Attribution License (CC BY). The use, distribution or reproduction in other forums is permitted, provided the original author(s) and the copyright owner(s) are credited and that the original publication in this journal is cited, in accordance with accepted academic practice. No use, distribution or reproduction is permitted which does not comply with these terms.